Extent and relevance of stacking disorder in "ice I_c"

Werner F. Kuhs[a,1], Christian Sippel[a,b], Andrzej Falenty[a], and Thomas C. Hansen[b]

[a]GeoZentrumGöttingen Abteilung Kristallographie (GZG Abt. Kristallographie), Universität Göttingen, 37077 Göttingen, Germany; and [b]Institut Laue-Langevin, 38000 Grenoble, France

Edited by Russell J. Hemley, Carnegie Institution of Washington, Washington, DC, and approved November 15, 2012 (received for review June 16, 2012)

A solid water phase commonly known as "cubic ice" or "ice I_c" is frequently encountered in various transitions between the solid, liquid, and gaseous phases of the water substance. It may form, e.g., by water freezing or vapor deposition in the Earth's atmosphere or in extraterrestrial environments, and plays a central role in various cryopreservation techniques; its formation is observed over a wide temperature range from about 120 K up to the melting point of ice. There was multiple and compelling evidence in the past that this phase is not truly cubic but composed of disordered cubic and hexagonal stacking sequences. The complexity of the stacking disorder, however, appears to have been largely overlooked in most of the literature. By analyzing neutron diffraction data with our stacking-disorder model, we show that correlations between next-nearest layers are clearly developed, leading to marked deviations from a simple random stacking in almost all investigated cases. We follow the evolution of the stacking disorder as a function of time and temperature at conditions relevant to atmospheric processes; a continuous transformation toward normal hexagonal ice is observed. We establish a quantitative link between the crystallite size established by diffraction and electron microscopic images of the material; the crystallite size evolves from several nanometers into the micrometer range with progressive annealing. The crystallites are isometric with markedly rough surfaces parallel to the stacking direction, which has implications for atmospheric sciences.

atmospheric ice | stacking faults | water frost | cirrus clouds | noctilucent clouds

It is generally assumed that there are two topologically different crystalline ambient pressure forms of water ice. Diffraction methods have played a crucial role for the identification of what has been called cubic ice or ice I_c, as most of its physical properties are quite similar to the common hexagonal form of ice, ice I_h (1, 2). Indeed, the free-energy difference between ice I_h and ice I_c is quite small (3) and varies notably depending on the exact formation conditions (4). This material is not a well-defined phase (1, 2) and is still not fully characterized.

The structure of ice I_h can be considered as a regular $[ABABAB]_\infty$ stacking of hexagonal symmetry by centering a structural building block at the midpoint of a H bond along the hexagonal *c* axis. Correspondingly, ideal ice I_c forms a cubic $[ABCABC]_\infty$ stacking of such building blocks (consisting of two H-bonded water molecules) centered at the midpoint of a H bond along a cubic 111 direction; both stacking arrangements are shown in Fig. 1.

It was noticed early on that ice formed by condensing water vapor on a cold support was not pure cubic ice (5). A number of attempts were made to explain the origin of the hexagonal features in the diffraction patterns and it was realized that there is a gradual transition from this defective ice I_c into well-crystallized ice I_h upon temperature increase. This transient phase has been given various names: cubic ice (sometimes so-called "cubic ice") or "ice I_c" (respectively, "ice Ic") are the most frequently used. We shall use the term "ice I_c" in the following; the quotation marks reflect the observational fact that there are deviations from cubic symmetry. The transition temperature range of "ice I_c" differs, partly owing to differences in the sensitivity of the method used for detection (1, 4). A suggestion by Kuhs et al. (6) set the correct entry point by explaining all deviations from a hypothetical perfectly cubic ice I_c, as manifested in the diffraction pattern, in terms of stacking faults. Other authors took up the idea and attempted to quantify the stacking disorder (7, 8). The most general approach to stacking disorder so far has been proposed by Hansen et al. (9, 10), who defined hexagonal (*H*) and cubic stacking (*K*) and considered interactions beyond next-nearest *H*- or *K* sequences. We shall discuss which interaction range needs to be considered for a proper description of the various forms of "ice I_c" encountered.

König identified what he called cubic ice 70 y ago (11) by condensing water vapor to a cold support in the electron microscope. A phase with cubic diffraction signatures can also be formed by heating the amorphous water phase (e.g., refs. 12, 13) from water freezing in silica mesopores (e.g., ref. 14), freezing of gels (15), aqueous ionic (16) or aqueous molecular solutions (17–19), from hyperquenched micrometer-sized water droplets (4), emulsified subcooled water (20), or by heating various high-pressure phases of ice recovered to ambient pressure (e.g., refs. 21, 22). "Ice I_c" may also be obtained by decomposing gas hydrates (23–26). Sample size (i.e., droplet- or pore size) plays an important role in many of these transitions; the formation of "ice I_c" is favored in nanometer-sized confined geometry, where it may take place directly from water up to temperatures close to melting. All transitions starting from a solid water phase leading to "ice I_c" were found to be irreversible. Fig. 2 shows the main established routes for forming "ice I_c".

We are not aware of any unequivocal diffraction observations of ice I_h, forming by any of the pathways shown in Fig. 2, for temperatures below ~190 K. Initially, stacking-disordered "ice I_c" forms and anneals toward ice I_h at an increased rate as temperature rises. The unambiguous assignment of the degree of stacking disorder requires good-quality diffraction data. Differences with respect to ice I_h are small, in the range from 200 to 240 K, and easily unnoticed in lower-resolution, lower-quality data.

There is general agreement, from diffraction as well as scanning electron microscopy (SEM), that "ice I_c" crystallites are of nanoscopic size upon formation. From diffraction peak broadening, typical sizes of 4–200 nm are deduced (e.g., refs. 6, 7), and there is some evidence that these small particles are isotropic (10). The smallness of ice crystals and their isotropic nature are likely to be at the base of cryopreservation methods for biological tissue (e.g., ref. 27). In the following we establish a quantitative link between crystallite sizes derived from cryo-SEM and diffraction.

The formation of ice in the Earth's atmosphere takes place predominantly at or in aerosol particles by either homogeneous (28, 29) or heterogeneous nucleation (30). Laboratory experiments have shown that aerosol droplets may form "ice I_c" at

Author contributions: W.F.K. and T.C.H. designed research; W.F.K., C.S., A.F., and T.C.H. performed research; C.S., A.F., and T.C.H. analyzed data; and W.F.K. and C.S. wrote the paper.

The authors declare no conflict of interest.

This article is a PNAS Direct Submission.

Freely available online through the PNAS open access option.

[1]To whom correspondence should be addressed. E-mail: wkuhs1@gwdg.de.

This article contains supporting information online at www.pnas.org/lookup/suppl/doi:10.1073/pnas.1210331110/-/DCSupplemental.

PHYSICS

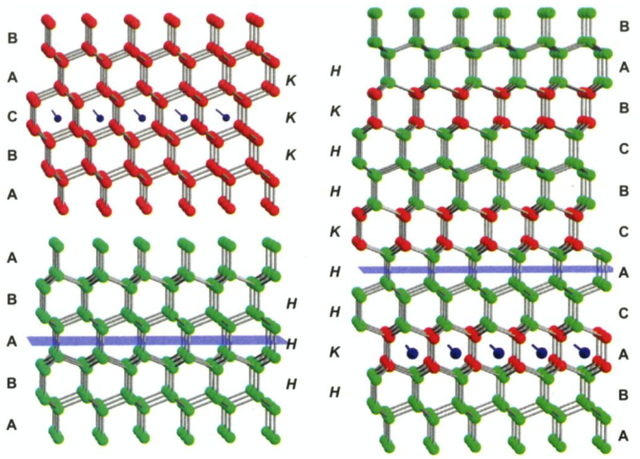

Fig. 1. (*Left*) Sequences of cubic (*Upper*) and hexagonal (*Lower*) stacking corresponding to the fault-free structures of ice I_c and ice I_h, respectively, in a ball-and-stick model; only the oxygen atoms are shown, which are connected by H bonds. The midpoints of the H bonds along the vertical stacking direction correspond to the topological A, B, and C layers of the stacking as indicated. Note that there is a horizontal mirror plane at the A and B locations in the case of ice I_h and an inversion center (on the arrows) at all locations A, B, and C in the case of ice I_c. Considering the local symmetries, one can define hexagonal *H*- and cubic *K* sequences with either a local mirror plane or a plane containing local inversion centers, respectively: any layer neighbored by two different layers, e.g., ABC, defines a *K* sequence; any layer surrounded by two identical layers, e.g., ABA, defines an *H* sequence. (*Right*) Example of a stacking-disordered arrangement of A, B, and C layers. Pairs of H-bonded water molecules along the stacking direction form a layer and possess either a local mirror symmetry (*H* stacking, green atoms, also represented as plane) or a local inversion center (*K* stacking, red atoms, also represented as arrows).

temperatures ≤ 235 K (8, 20). The following growth of ice crystals is governed by vapor deposition of water molecules on the initially very small particles evolving well into the micrometer scale (28); the latter process takes place typically on a minute-to-hour scale for cirrus clouds (28, 31). Moreover, the high water vapor supersaturation observed in cirrus clouds and contrails (e.g., ref. 32) may be due to the presence of "ice I_c" with its higher vapor pressure (33), among other possible explanations (31, 34). Observations on snow crystal morphologies (35) suggest that in some cases, starting from an apparently cubic nucleus, hexagonal crystals may grow from the vapor phase along the cubic [111] directions, thus forming multiple twins. It is unclear how frequently this happens and to what extent cubic stacking sequences are formed directly from the vapor phase. Experimentally, it has been established that thin vapor-deposited films of ice anneal to "ice I_c" (36, 37). In the following, we present details of the microstructural evolution of vapor-deposited ice at temperatures from 175 to 240 K over many hours, i.e., at timescales relevant to the processes in the Earth's atmosphere.

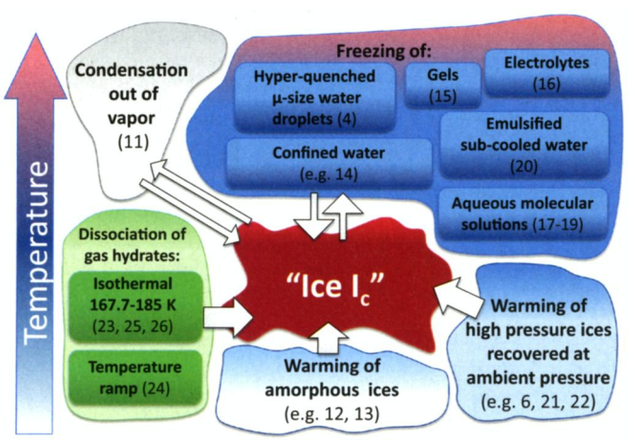

Fig. 2. Main established routes of forming "ice I_c".

Results

Time-Resolved Neutron Diffraction Study of "Ice I_c". The crystallographic details of "ice I_c" formed from the vapor phase or by isothermal decomposition of gas hydrates have been studied by neutron diffraction at the high-intensity two-axis diffractometer D20 (38) at the High-Flux Reactor of the Institut Laue-Langevin in Grenoble, France (*Methods*).

The diffraction data obtained show clear signs of stacking disorder as well as diffraction broadening due to small crystallite sizes, both changing with time and temperature. The complex diffraction patterns clearly cannot be explained by a simple mixture of the pure ice I_c and ice I_h phases; they were analyzed by means of a least-squares full-pattern profile refinement using the stacking disorder model of some of us (9, 10). For a satisfactory description, interactions up to the next-nearest layer had to be introduced, leading to four independent parameters α, β, γ, and δ corresponding to an interaction range $s = 4$ (*SI Text*). Using this model, a very satisfactory agreement between experimental observation and the model was obtained in all investigated cases; the introduction of amorphous components (16, 39) was not necessary to obtain a good fit. In particular, at lower and intermediate temperatures the complex stacking-disordered nature of "ice I_c" cannot be fully captured in the model set up by Malkin et al. (8) and computed with DIFFaX (40). In *SI Text* we give the relation between this simpler model and our more general approach; we also show how important it is to extend the modeling of stacking disorder to $s = 4$. "Ice I_c" is characterized by a complex sequence of layers with preferences for one or another of the possible stacking probabilities α, β, γ, and δ (*SI Text*). In all our experiments the mix of these variants appears to be very reproducible for a given formation route as already shown for "ice I_c" obtained from recovered high-pressure phases of ice (9, 10); furthermore, there is a systematic variation of the four stacking-fault parameters as a function of annealing time. From these parameters, both the "cubicity" (i.e., the fraction of cubic stacking sequences) and the faulting probabilities Φ_c and Φ_h (8) can be calculated (*SI Text*). Only at the highest investigated temperatures is the much simpler $s = 2$ model capable of describing the diffraction data; such a high-temperature case was studied in Malkin et al. (8) for the homogeneous nucleation of micrometer-sized water droplets near 232 K.

The ongoing changes in terms of the stacking disorder and crystallite size were established by a sequential analysis of several thousand complete neutron diffraction data sets as a function of temperature (and time) as well as isothermally as a function of time. Fig. 3 shows the time-dependent decrease of cubicity for different temperatures. A monotonic decrease of the proportion of cubic sequences is observed taking place very slowly at 175 K, on a time scale of several hours at 180 K, and twice as fast at 185 and 190 K. However, even at the highest temperatures investigated, a full transformation into pure ice I_h is not observed; a significant fraction (a few percent) of cubic stacking sequences remains, with very little further decay in the investigated time frame. The influence of temperature on the rate of transformation into hexagonal ice is also clearly seen in temperature-ramping experiments. Whereas some changes toward ice I_h take place at temperatures as low as 140 K, a clear acceleration is seen in the temperature range of 180–185 K with a rapid

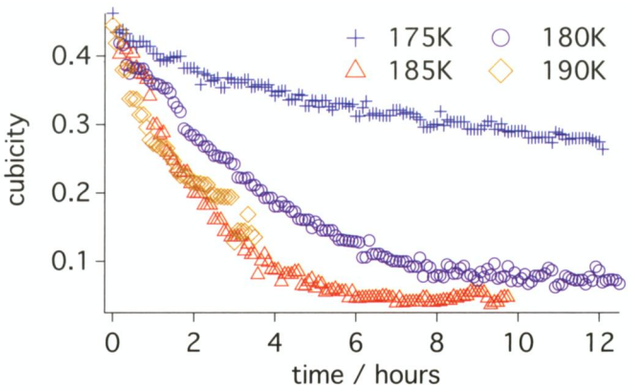

Fig. 3. Evolution of cubicity as a function of time for annealing of vapor-deposited frost at temperatures of 175, 180, 185, and 190 K. Compared with 175 K, a clear acceleration of the loss of cubic sequences is seen at 180 K, speeding up even more at 185 K, whereas a smaller further change is seen at 190 K.

conversion into a rather hexagonal appearance (see details in *SI Text*). However, even at 210 K, some cubic stacking sequences persist, disappearing only upon heating to 240 K. The fact that a fraction of cubic sequences persists up to almost 240 K was noticed earlier (23) and is in agreement with the extended temperature range of the transformation into ice I_h, as observed by differential thermal analysis (4). The accumulated evidence leaves very little doubt that the changes observed by earlier thermal analysis and diffraction work are related to the progressively disappearing cubic components in the stacking.

In all cases we are quite far from a random stacking situation, where all four distinct stacking probability parameters α, β, γ, and δ would converge to the same value (*SI Text*). Moore and Molinero (41) had suggested that the nonrandom stacking signatures are a result of kinetic factors during formation from the liquid. For the growth on substrates from the gas phase, Thürmer and Bartelt (42) have found screw dislocations at the origin of cubic stacking sequences. One would expect a high proportion of δ sequences in the case where this is the dominant formation mechanism for our vapor-deposited samples. However, δ usually does not exceed values of about 0.7; this means that the screw dislocation mechanism is not the only one at work in our case. There is good evidence that the nonrandom correlations in the stacking sequences are characteristic for a certain preparation path and may well be reflecting topological relations of the water molecular arrangements in the parent phase (*SI Text*). A possible molecular mechanism for the formation of stacking faults involving pairs of point defects was recently established from computer simulations (43) and certainly merits further consideration.

The diffraction broadening due to crystallite size effects is an intrinsic part of the model used in our work. It takes into account variations of the mean crystallite size, if necessary, in two independent directions parallel and perpendicular to the stacking axis (9). The decrease in cubicity with time and temperature was accompanied by an increase of the mean crystallite size (*SI Text*). Because the total amount of sample was kept constant during the experiments, the apparent increase of mean size (as reflected in the sharpening of the Bragg reflections) must be ascribed to larger crystallites that had grown at the expense of smaller ones. The likely processes are a differential sublimation and recondensation at the crystallite surface (Ostwald ripening) as well as a local water molecule migration across grain boundaries (normal grain growth). Both processes are expected to speed up with higher temperature as a consequence of the activated nature of water mobility. However, complications may arise from the nucleation of less-defective crystals in a process known in material science as recovery–recrystallization. This process may even temporarily reduce the crystallite size as observed for the 180 K run (*SI Text*). The nucleation of less-defective crystallites as part of the complex transitions of stacking-disordered ice toward ice I_h was already proposed by Hansen et al. (10) on the basis of small-angle neutron scattering experiments and finds further support here. There is, however, no evidence from our data that recovery–recrystallization is the dominant annealing process. The complexity of the annealing toward ice I_h is reflected in the observation that there is no simple correlation between the decreasing cubicity and an increasing crystallite size. Whereas crystallite growth drives well at both 175 and 180 K, the stacking rearrangements are considerably slower at the lower temperature. This is not surprising, considering the possible mechanisms involved. Crystal coarsening needs single mobile water molecules at the surface or interface, which in the temperature range of interest certainly is high enough for sublimation–condensation-driven processes (44). On the other hand, the progressive transformation of the bulk into the new topological arrangement of ice I_h within a crystallite must involve molecular reorientations likely to be supported by migrating orientational defects of water molecules, i.e., activated mobile Bjerrum defects (45).

SEM. The starting material of the diffraction experiments, as well as samples recovered after the neutron diffraction runs, were studied by SEM (*Methods*). Fresh samples of vapor-deposited ice (frost) were found to consist of spherulitic agglomerates of micrometer-sized units, which in turn are composed of aggregated largely isometric nanoparticles (Fig. 4); their size ranges from ~50 to 200 nm. SEM has repeatedly been used to study vapor-deposited ice; we have clearly identified the smallest units within this hierarchical structure. This microstructure is reproducibly formed in all our vapor-deposition experiments and a diffraction analysis of these samples reveals the marked stacking disorder of this material. The crystallite size derived from our stacking model (9) yields sizes in the same range; thus, we conclude that the smallest particles seen by SEM are indeed crystallites (and not polycrystalline aggregates). The nanoparticles appear to touch each other but do not seem to form a compact mass. Whether the presence of voids between the crystallites is a general feature in the bulk of stacking-disordered ice cannot be firmly stated at present. However, the high contrast of "ice I_c" formed from recovered high-pressure ices as evidenced in small-angle neutron scattering experiments (10) suggests a similar situation. Arguments for the extended transition range of "ice I_c" into ice I_h drawn from grain-boundary and strain energies between the crystallites (46) will certainly not be applicable to the loosely connected aggregates of vapor-deposited ice. Samples recovered at the end of the isothermal diffraction experiments show indeed

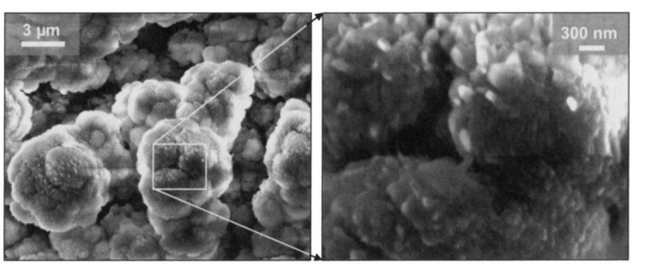

Fig. 4. SEM micrographs showing the hierarchic microstructure of vapor-deposited water frost. (*Left*) Micrometer-sized spherules consisting of smaller units, which themselves consist of more or less isometric nanoparticles (*Right*); their sizes correspond to the crystallite size established by analyzing diffraction data of the same sample.

a largely unchanged hierarchical structure with some coarsening in the substructure in agreement with the slight increase of crystallite size established by diffraction, but also a somewhat larger size of the aggregated nanoparticles. This coarsening is likely to happen as a consequence of sublimation–condensation cycles (44) of water molecules involving diffusive transport across the void space.

The SEM micrographs of "ice I_c" obtained from decomposing CO_2 hydrates show individual stacking-faulty crystals, too. By the end of the isothermal neutron diffraction experiments, which were several hours long, some of them had grown into micrometer-sized crystals of pseudohexagonal symmetry (Fig. 5). Remarkably, the faceted crystals show kinks in the prismatic planes; they can only be ascribed to the stacking disorder seen in the diffraction experiments on the same material. There is good evidence that the number of kinks becomes smaller at higher temperature, i.e., at lower cubicity of the stacking. The stacking planes seem to extend over the complete diameter of the crystal; this is in contrast with stacking faults in ice I_h crystals which often are confined to a certain section of the single crystal (47). Stacking disorder thus produces considerable additional surface roughness of the crystallites in line with earlier observations (48); this will likely affect their light-scattering properties in cirrus clouds (49, 50). Moreover, the rough surface with multiple kinks seen in our electron micrographs is likely to influence the water condensation and evaporation kinetics (51), as well as the uptake of foreign molecular species (32). Water uptake coefficient on vapor-deposited ice (51) has a temperature dependency very similar to the evolution of cubicity; both cubicity and uptake coefficient slowly decrease upon approaching 180 K and show an accelerated decrease up to ~205 K before leveling at low values at higher temperatures. Undoubtedly, the peculiar surface properties of "ice I_c" merit further investigations to elucidate their role in ice growth and uptake kinetics in cirrus clouds.

Discussion

Considerable efforts have been made in recent years to better understand the formation and complex microstructural changes of "ice I_c" during its transformation to ice I_h. Our model of stacking disorder presents the pertinent features of the stacking disorder. The arrangement is generally not random but characterized by specific sequences involving topological preferences between nearest- and even next-nearest neighboring layers. Typically four parameters are needed to describe the stacking disorder. The parameter mix translates into a diffraction pattern providing the fingerprint for the specific form of "ice I_c" obtained from a given parent phase. Once crystallized, "ice I_c" keeps changing as a function of both time and temperature for all its existence. Some generalities emerge from our observations: (*i*) The cubicity monotonically decreases with annealing time and increasing temperature. This clearly shows that it is the hexagonal stacking order that is preferred thermodynamically. (*ii*) The annealing accelerates at ~180 K, leading to an almost hexagonal crystal within a few hours. The activation energies of the transformation have been measured (52) and were found to change in this temperature range (from 21.4 kJ/mol below to 44.8 kJ/mol above). Unfortunately, the underlying processes remain obscure and will not be pinned down easily. (*iii*) Some stacking disorder (several percent cubic stacking sequences) remains at temperatures above 200 K and easily persists up to ~240 K. Undoubtedly, all ice crystals formed at temperatures below ~190 K undergo complex microstructural changes with time and upon warming. (*iv*) The lattice constants and their deduced ratios (c/a) of "ice I_c" and ice I_h are distinctly different, indicating some small differences in the long-ranged molecular interactions (*SI Text*). We note in this context that a closer inspection of published data of ice formed below ~240 K often shows deviations from good hexagonal ice—most noticeable in the hexagonal (002) powder peak, which has a higher intensity than expected for ice I_h. This becomes most evident in a crystallographic full-pattern Rietveld analysis (23). Ice samples obtained in the temperature range from 190 to 240 K merit close attention in this respect.

Electron microscopy provides additional microstructural insights: Firstly, we have established a link between the microscopic observation and the crystallite size obtained from diffraction data. There is reasonable agreement when considering the fact that diffraction broadening is calculated under the assumption of monodisperse crystallites. Secondly, it appears that "ice I_c" crystallites are more or less isometric, developing trigonal or pseudohexagonal shapes when facets emerge as size increases. Thirdly, the prismatic planes of these crystals show numerous kinks, likely related to the stacking disorder.

We now comment on some astrophysical implications of our results. In moderately cold (~130–190 K) astrophysical and planetary environments, "ice I_c" is considered to be by far the most likely form of condensed water (1, 2). Jenniskens and Blake

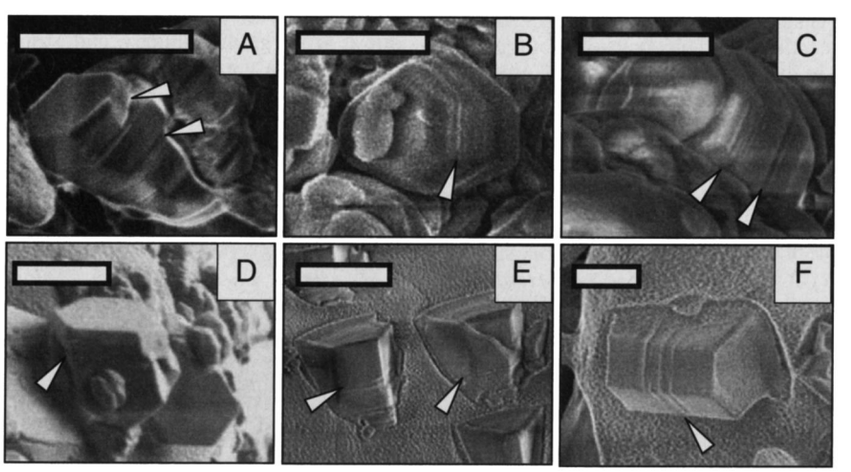

Fig. 5. SEM micrographs of single crystallites of "ice I_c" formed by decomposition of CO_2 hydrates via a sudden depressurization to gas pressure well below the hydrate stability. Formation conditions: (*A*) 167.7 K and 6 mbar, (*B*, *C*) 175 K and 6 mbar, (*D*) 195 K and 6 mbar, (*E*, *F*) 220 K and 900 mbar. Scale bar: 5 μm. All crystallites have a pseudohexagonal shape and have kinks (some indicated by white arrows) on the prismatic faces. Whereas at the lowest temperatures kinks are frequent and the prismatic planes quite rough, at the highest temperatures larger portions of the prismatic planes are free of kinks.

(43) have suggested the persistence of amorphous components in ice (partly) crystallized from the amorphous phase by heating. This hypothesis is strongly anchored in the astrophysical community, which refers to the amorphous component for its better solubility of gaseous components. In contrast, the ice physics community has found no compelling evidence for important residual amorphous contribution at temperatures higher than ~160 K (53). Some molecular-scale computer simulations of the freezing of supercooled water (41, 54) support the experimental finding of a coexistence of "ice I_c" and amorphous ice. It is, however, an open question whether (and how much of) the solidified water remains amorphous at longer experimental timescales. The large portion (~20%) of residual amorphous contribution found in computer simulations (41) may simply be due to the incomplete annealing achieved within the accessible microsecond timescale; however, it cannot be excluded that this difference may be due to the different pathway of formation. From our diffraction studies we now find that significant amounts of amorphous phase are unlikely to exist in contact with "ice I_c"; earlier evidence for amorphous relics in "ice I_c", based on a simplified analysis of low-resolution diffraction data (16, 39, 43), should be reconsidered in the light of an appropriate model for stacking disorder and with higher-resolution data, in line with the conclusions of Mitlin and Leung (53). The situation may, however, be different for solutes at high concentration, which impede or even prevent any water crystallization at temperatures even far below the melting point (55).

Numerous references are made to "ice I_c" in atmospheric science, in particular in the context of cirrus clouds (20, 31, 33, 56, 57). The possible presence of "ice I_c" is generally considered in the short life cycles of such clouds and has been studied in some detail in laboratory work (8, 20, 33, 55, 58, 59) and molecular-scale computer simulations of freezing of supercooled water (8, 60–62). Although our experimental results for the increasing particle size in the densely packed samples investigated (as a consequence of the intercrystallite mass transfer) cannot be transferred directly to atmospheric conditions, the changes of stacking disorder are intrinsic to the particle and can be expected to take place also in clouds. The following findings are particularly relevant: (*i*) Our SEM results show that the morphology of crystallites of stacking-disordered ice is often trigonal or pseudohexagonal. Such trigonal crystals have been observed in cirriform clouds (63); triangular growth morphologies were also found in molecular simulations (62). Clearly, a pseudohexagonal crystal shape cannot be taken as evidence for ice I_h (23). (*ii*) Our diffraction data show that crystals of "ice I_c" may exist up to ~240 K in the atmosphere. (*iii*) Our SEM results show that the surfaces of crystals of "ice I_c" have a higher roughness compared with ice I_h; for larger crystals kinks are developed on the prismatic planes in a systematic manner and may also form under atmospheric conditions with likely consequences for surface reactivity (32). More work is needed to establish the degree of cubicity and the particle-size distribution of stacking-disordered ice formed in the atmosphere (56). With the knowledge of particle number and surface roughness, the light-scattering behavior in the atmosphere can be estimated (50, 64–66). This is important, as the backscattering properties of cirrus clouds are one of the major unknowns to quantify the Earth's radiation balance (e.g., ref. 65). Moreover, we reemphasize our earlier statement that there is no singular diffraction evidence that ice I_h has formed below ~190 K. Consequently, one has to expect that the crystalline water phase formed in the colder parts of the Earth's atmosphere is at least initially "ice I_c". Likewise, "ice I_c" can be predicted to be found in noctilucent clouds, in which temperatures go down to ~130 K (67, 68).

Conclusions

What has been called "cubic ice" or "ice I_c" for 70 y now turns out to be arguably the most faceted ice phase in a literal and a more general sense. We have presented some of its pertinent microstructural characteristics affecting the molecular arrangements in the bulk as well as the surface characteristics of this ubiquitous low-temperature, ambient pressure form of water ice, resulting in important differences between "ice I_c" and ice I_h. More work remains to be done to elucidate the formation mechanisms as well as the detailed implications of the stacking disorder of "ice I_c", e.g., concerning the incorporation of impurities, the possible role of defect sites in promoting chemical reactivity, and the resulting physical properties (such as vapor pressure); all these features are of considerable interest in particular in atmospheric and planetary sciences.

Methods

Sample Preparation. Samples of vapor-deposited "ice I_c" ("frost") were prepared by condensing deuterated water vapor onto a copper disk half-immersed in liquid N_2 rotating at 0.5 Hz. The deposited material was mechanically removed at regular intervals (a few seconds), collected, and stored in liquid N_2 for later use. Diffraction data of the recovered material show the presence of "ice I_c" without major contributions of an amorphous phase.

In another series of experiments, "ice I_c" was obtained in situ on the neutron diffractometer from decomposing deuterated CO_2 hydrates by adjusting within seconds the gas atmosphere to values below hydrate stability at controlled constant temperature; see also Falenty and Kuhs (25).

Neutron Diffraction Experiments. These were carried out on the high-intensity two-axis diffractometer D20 (38) at the high-flux reactor of the Institut Laue-Langevin using a wavelength of 2.42 Å. The instrument was used in its highest flux configuration at a take-off angle of 42° from a vertically focusing highly oriented pyrolytic graphite monochromator with additional Soller collimation in the primary beam to improve angular resolution. Samples were kept in a helium flow cryostat ("orange cryostat") at temperatures controlled within a fraction of a kelvin of the desired value. All samples were recovered at the end of the experiments by a rapid quench to liquid N_2 temperatures for further inspection by SEM.

Scanning Electron Microscopy. An FEI Quanta 200F and an LEO 1530 Gemini instrument equipped with Polaron and Oxford CTH1500HF cryostages, respectively, were used for SEM investigations. The uncoated samples were studied at about 90 K (with liquid N_2 as coolant) and a pressure of about 0.1 Pa. To minimize sample deterioration in the electron beam, a fairly low acceleration voltage of 2.5 keV was used. Only insignificant alterations of the sample surface were observed over the inspection period of up to 1 h.

ACKNOWLEDGMENTS. We thank Michael Koza (Institut Laue-Langevin, Grenoble) for fruitful discussion and the Institut Laue-Langevin for beam time and support. We also acknowledge a 3-y doctoral studentship from ILL (to C.S.). The study was financially supported by the Deutsche Forschungsgemeinschaft, Grant Ku920/11.

1. Hobbs PV (1974) *Ice Physics* (Oxford Univ Press, Oxford).
2. Petrenko V, Withworth R (1999) *Physics of Ice* (Oxford Univ Press, Oxford).
3. Handa YP, Klug DD, Whalley E (1986) Difference in energy between cubic and hexagonal ice. *J Chem Phys* 84(12):7009–7010.
4. Kohl I, Mayer E, Hallbrucker A (2000) The glassy water-cubic ice system: A comparative study by X-ray diffraction and differential scanning calorimetry. *Phys Chem Chem Phys* 2(8):1579–1586.
5. Shallcross FV, Carpenter GB (1957) X-ray diffraction study of the cubic phase of ice. *J Chem Phys* 26(4):782–784.
6. Kuhs WF, Bliss DV, Finney JL (1987) High-resolution neutron powder diffraction study of ice I_c. *J Phys Colloq* 48(C-1):631–636.
7. Morishige K, Uematsu H (2005) The proper structure of cubic ice confined in mesopores. *J Chem Phys* 122(4):4.
8. Malkin TL, Murray BJ, Brukhno AV, Anwar J, Salzmann CG (2012) Structure of ice crystallized from supercooled water. *Proc Natl Acad Sci USA* 109(4):1041–1045.
9. Hansen T, Koza MM, Kuhs WF (2008) Formation and annealing of cubic ice: I. Modelling of stacking faults. *J Phys Condens Matter* 20(28):285104, 12 pp.
10. Hansen T, Koza MM, Lindner P, Kuhs WF (2008) Formation and annealing of cubic ice: II. Kinetic study. *J Phys Condens Matter* 20(28):285105, 14 pp.
11. König H (1943) Eine kubische Eismodifikation. *Z Kristallogr* 105(4):279–286.
12. Dowell LG, Rinfret AP (1960) Low-temperature forms of ice as studied by x-ray diffraction. *Nature* 188(4757):1144–1148.

PHYSICS

13. Mcmillan JA, Los SC (1965) Vitreous ice: Irreversible transformations during warm-up. *Nature* 206(4986):806–807.
14. Baker JM, Dore JC, Behrens P (1997) Nucleation of ice in confined geometry. *J Phys Chem B* 101(32):6226–6229.
15. Dowell LG, Moline SW, Rinfret AP (1962) A low-temperature x-ray diffraction study of ice structures formed in aqueous gelatin gels. *Biochim Biophys Acta* 59(1):158–167.
16. Elarby-Aouizerat A, Jal JF, Dupuy J, Schildberg H, Chieux P (1987) Comments on the ice I_c structure and I_c to I_h phase transformation mechanism: A neutron scattering investigation of ice precipitates in glassy LiCl·D2O. *J Phys Colloq* 48(C-1):465–470.
17. Vigier G, Thollet G, Vassoille R (1987) Cubic and hexagonal ice formation in water-glycerol mixture (50% w/w). *J Cryst Growth* 84(2):309–315.
18. Kajiwara K, Thanatuksom P, Murase N, Franks F (2008) Cubic ice can be formed directly in the water phase of vitrified aqueous solutions. *Cryo Lett* 29(1):29–34.
19. Palacios ODC, Inaba A, Andersson O (2010) Low-temperature heat capacity of a two-dimensionally ordered structure of ice crystallized from glycerol aqueous solutions. *Thermochim Acta* 500(1-2):106–110.
20. Murray BJ, Knopf DA, Bertram AK (2005) The formation of cubic ice under conditions relevant to Earth's atmosphere. *Nature* 434(7030):202–205.
21. Arnold GP, Finch ED, Rabideau SW, Wenzel RG (1968) Neutron-diffraction study of ice polymorphs. III. Ice Ic. *J Chem Phys* 49(10):4354–4369.
22. Bertie JE, Calvert LD, Whalley E (1963) Transformations of ice II, ice III, and ice V at atmospheric pressure. *J Chem Phys* 38(4):840–846.
23. Kuhs W, Genov G, Staykova D, Hansen T (2004) Ice perfection and onset of anomalous preservation of gas hydrates. *Phys Chem Chem Phys* 6(21):4917–4920.
24. Takeya S, et al. (2005) Particle size effect of CH_4 hydrate for self-preservation. *Chem Eng Sci* 60:1383–1387.
25. Falenty A, Kuhs WF (2009) "Self-preservation" of CO_2 gas hydrates—surface microstructure and ice perfection. *J Phys Chem B* 113(49):15975–15988.
26. Falenty A, Hansen T, Kuhs WF (2011) Cubic ice formation and annealing from CO_2 clathrate hydrate decomposition at low temperatures. *Physics and Chemistry of Ice 2010*, eds Furukawa Y, Sazaki G, Uchida T, Watanabe N (Hokkaido Univ Press, Sapporo), pp 411–419.
27. Uchida T, Takeya S, Nagayama M, Gohar K (2012) *Crystallization and Materials Science of Modern Artificial and Natural Crystals*, ed Borisenko E (InTech, New York, Shanghai, Rijeka), pp 203–224.
28. Kärcher B (2002) Properties of subvisible cirrus clouds formed by homogeneous freezing. *Atmos Chem Phys* 2:161–170.
29. Koop T (2004) Homogeneous ice nucleation in water and aqueous solutions. *Z Phys Chem* 218(11):1231–1258.
30. Kärcher B, Lohmann U (2003) A parameterization of cirrus cloud formation: Heterogeneous freezing. *J Geophys Res Atmos* 108(D14):15.
31. Peter T, et al. (2006) Atmosphere. When dry air is too humid. *Science* 314(5804): 1399–1402.
32. Gao RS, et al. (2004) Evidence that nitric acid increases relative humidity in low-temperature cirrus clouds. *Science* 303(5657):516–520.
33. Shilling J, et al. (2006) Measurements of the vapor pressure of cubic ice and their implications for atmospheric ice clouds. *Geophys Res Lett* 33(17):5.
34. Krämer KW, et al. (2009) Ice supersaturations and cirrus cloud crystal numbers. *Atmos Chem Phys* 9(11):3505–3522.
35. Kobayashi T, Kuroda T (1987) *Morphology of Crystals*, ed Sunagawa I (Terra Science Publishing, Tokyo), pp 645–673.
36. Ruan CY, Lobastov VA, Vigliotti F, Chen S, Zewail AH (2004) Ultrafast electron crystallography of interfacial water. *Science* 304(5667):80–84.
37. Yang D-S, Zewail AH (2009) Ordered water structure at hydrophobic graphite interfaces observed by 4D, ultrafast electron crystallography. *Proc Natl Acad Sci USA* 106(11):4122–4126.
38. Hansen T, Henry PF, Fischer HE, Torregrossa J, Convert P (2008) The D20 instrument at the ILL: A versatile high-intensity two-axis neutron diffractometer. *Meas Sci Technol* 19(3):6.
39. Seyed-Yazdi J, Farman H, Dore JC, Webber JB, Findenegg GH (2008) Structural characterization of water/ice formation in SBA-15 silicas: III. The triplet profile for 86 Å pore diameter. *J Phys Condens Matter* 20(20):205108, 12 pp.
40. Treacy MMJ, Newsam JM, Deem MW (1991) A general recursion method for calculating diffracted intensities from crystals containing planar faults. *Proc R Soc London, Ser A* 433(1889):499–520.
41. Moore EB, Molinero V (2011) Is it cubic? Ice crystallization from deeply supercooled water. *Phys Chem Chem Phys* 13(44):20008–20016.
42. Thürmer K, Bartelt NC (2008) Growth of multilayer ice films and the formation of cubic ice imaged with STM. *Phys Rev B* 77(19):195425.
43. Jenniskens P, Blake DF (1996) Crystallization of amorphous water ice in the solar system. *Astrophys J* 473(2):1104–1113.
44. Pratte P, van den Bergh H, Rossi MJ (2006) The kinetics of H_2O vapor condensation and evaporation on different types of ice in the range 130-210 K. *J Phys Chem A* 110(9):3042–3058.
45. Wooldridge PJ, Richardson HH, Devlin JP (1987) Mobile Bjerrum defects - A criterion for ice-like crystal-growth. *J Chem Phys* 87(7):4126–4131.
46. Johari GP (1998) On the coexistence of cubic and hexagonal ice between 160 and 240 K. *Philos Mag B* 78(12BIS):375–383.
47. Ogura M, Hondoh T (1988) *Lattice Defects in Ice Crystals*, ed Higashi A (Hokkaido Univ Press, Sapporo), pp 49–67.
48. Kobayashi T, Ohtake T (1974) Hexagonal twin prisms of ice. *J Atmos Sci* 31(5): 1377–1383.
49. Schnaiter M, Kaye PH, Hirst E, Ulanowski Z, Wagner R (2011) Exploring the surface roughness of small ice crystals by measuring high resolution angular scattering patterns. *AAPP | Physical, Mathematical, and Natural Sciences* 89(Suppl N°1): C1V89S1P084.
50. Ulanowski Z, Kaye P, Hirst E, Greenaway RS (2010). Light scattering by ice particles in the Earth's atmosphere and related laboratory measurements. *12th Conference on Electromagnetic and Light Scattering*, eds Muinonen K, Penttilä A, Lindquist H, Nousiainen T, Videen G (University of Helsinki, Helsinki), pp 294–297.
51. Delval C, Rossi MJ (2004) The kinetics of condensation and evaporation of H_2O from pure ice in the range 173-223 K: A quartz crystal microbalance study. *Phys Chem Chem Phys* 6(19):4665–4676.
52. Sugisaki M, Suga H (1968) Calorimetric study of the glassy state. IV. Heat capacities of glassy water and cubic ice. *Bull Chem Soc Jpn* 41(11):2591–2599.
53. Mitlin S, Leung K (2002) Film growth of ice by vapor deposition at 128-185 K studied by Fourier transform infrared reflection-absorption spectroscopy: Evolution of the OH stretch and the dangling bond with film thickness. *J Phys Chem B* 106(24):6234–6247.
54. Moore EB, de la Llave E, Welke K, Scherlis DA, Molinero V (2010) Freezing, melting and structure of ice in a hydrophilic nanopore. *Phys Chem Chem Phys* 12(16): 4124–4134.
55. Murray BJ, Bertram AK (2008) Inhibition of solute crystallisation in aqueous $H(^+)$-NH_4 $(^+)$-$SO_4(^{2-})$-H_2O droplets. *Phys Chem Chem Phys* 10(22):3287–3301.
56. Murphy DM (2003) Dehydration in cold clouds is enhanced by a transition from cubic to hexagonal ice. *Geophys Res Lett* 30(23):2230.
57. Murray B, et al. (2010) Heterogeneous nucleation of ice particles on glassy aerosols under cirrus conditions. *Nat Geosci* 3(4):233–237.
58. Murray BJ, Bertram AK (2007) Strong dependence of cubic ice formation on droplet ammonium to sulfate ratio. *Geophys Res Lett* 34(16):L16810.
59. Murray BJ (2008) Enhanced formation of cubic ice in aqueous organic acid droplets. *Environ Res Lett* 3(2):025008.
60. Carignano M (2007) Formation of stacking faults during ice growth on hexagonal and cubic substrates. *J Phys Chem C* 111(2):501–504.
61. Brukhno A, Anwar J, Davidchack R (2008) Challenges in molecular simulation of homogeneous ice nucleation. *J Phys Condens Matter* 20(49):17.
62. Pirzadeh P, Kusalik PG (2011) On understanding stacking fault formation in ice. *J Am Chem Soc* 133(4):704–707.
63. Heymsfield A (1986) Ice particles observed in a cirriform cloud at -83°C and implications for polar stratospheric clouds. *J Atmos Sci* 43(8):851–855.
64. Kaye PH, et al. (2008) Classifying atmospheric ice crystals by spatial light scattering. *Opt Lett* 33(13):1545–1547.
65. Baran A (2009) A review of the light scattering properties of cirrus. *J Quant Spectrosc Radiat Transf* 110(14-16):1239–1260.
66. Hesse E, et al. (2012) Modelling diffraction by facetted particles. *J Quant Spectrosc Radiat Transf* 113(5):342–347.
67. Rapp M, Thomas GA, Baumgarten G (2007) Spectral properties of mesospheric ice clouds: Evidence for non-spherical particles. *J Geophys Res* 112(D3):19.
68. Baumgarten G, Fiedler J, Lübken FJ, van Cossart G (2008) Particle properties and water content of noctilucent clouds and their interannual variation. *J Geophys Res* 113(D6):13.